Chemistry & Biology
Article

Selective Positive Modulator of Calcium-Activated Potassium Channels Exerts Beneficial Effects in a Mouse Model of Spinocerebellar Ataxia Type 2

Adebimpe W. Kasumu,[1,5] Charlotte Hougaard,[3,5] Frederik Rode,[3] Thomas A. Jacobsen,[3] Jean Marc Sabatier,[4] Birgitte L. Eriksen,[3] Dorte Strøbæk,[3] Xia Liang,[1] Polina Egorova,[2] Dasha Vorontsova,[2] Palle Christophersen,[3,*] Lars Christian B. Rønn,[3,6] and Ilya Bezprozvanny[1,2,*]

[1]Department of Physiology, UT Southwestern Medical Center at Dallas, Dallas, TX 75390, USA
[2]LMN, St. Petersburg Polytechnical University, St. Petersburg 195251, Russia
[3]NeuroSearch A/S, Pederstrupvej 93, DK-2750 Ballerup, Denmark
[4]INSERM UMR 1097, Université d'Aix-Marseille, Parc Scientifique et Technologique de Luminy, 13288 Marseille Cedex 09, France
[5]These authors contributed equally to this work
[6]Present address: Lundbeck A/S, Ottiliavej 9, DK-2500 Valby, Denmark
*Correspondence: pc@neurosearch.com (P.C.), ilya.bezprozvanny@utsouthwestern.edu (I.B.)
http://dx.doi.org/10.1016/j.chembiol.2012.07.013

SUMMARY

Spinocerebellar ataxia type 2 (SCA2) is a neurodegenerative disorder caused by a polyglutamine expansion within the Ataxin-2 (Atxn2) protein. Purkinje cells (PC) of the cerebellum fire irregularly and eventually die in SCA2. We show here that the type 2 small conductance calcium-activated potassium channel (SK2) play a key role in control of normal PC activity. Using cerebellar slices from transgenic SCA2 mice we demonstrate that SK channel modulators restore regular pacemaker activity of SCA2 PCs. Furthermore, we also show that oral delivery of a more selective positive modulator of SK2/3 channels (NS13001) alleviates behavioral and neuropathological phenotypes of aging SCA2 transgenic mice. We conclude that SK2 channels constitute a therapeutic target for SCA2 treatment and that the developed selective SK2/3 modulator NS13001 holds promise as a potential therapeutic agent for treatment of SCA2 and possibly other cerebellar ataxias.

INTRODUCTION

Spinocerebellar ataxia type 2 (SCA2) belongs to the family of polyglutamine expansion (polyQ) disorders. This group of degenerative and hereditary diseases also comprises Huntington's disease (HD), dentatorubropallidoluysian atrophy (DRPLA), spinobulbar muscular atrophy (SBMA), and other SCAs, including SCA1, SCA3 (Machado-Joseph disease), SCA6, SCA7, and SCA17 (Carlson et al., 2009; Matilla-Dueñas et al., 2010; Orr and Zoghbi, 2007). In these polyQ disorders, an unstable CAG expansion within the disease-causing gene encodes an elongated polyQ tract, which is associated with a progressive neuronal degeneration accompanied by different clinical manifestations that depend on the function and expression pattern of the affected protein. A common feature of SCAs is a progressive cerebellar ataxia (Klockgether et al., 1998). In SCA2, disease pathogenesis is caused by polyQ expansion of more than 57 repeats in the ataxin-2 (Atxn2) protein (Pulst et al., 1996), the function of which is not well understood. Interestingly, polyQ repeat expansions of intermediate length in Atxn2 have been associated with amyotrophic lateral sclerosis (ALS) and parkinsonian symptoms (Ross et al., 2011; Simon-Sanchez et al., 2005). The cerebellar ataxia in SCA2 is associated with a loss of Purkinje cells (PCs) and generation of cytoplasmic inclusions (Huynh et al., 2000; Liu et al., 2009). The nuclear inclusion bodies characteristic of other polyQ disorders are not prominent in SCA2 (Huynh et al., 2000; Lastres-Becker et al., 2008). The reason for PC degeneration in SCA2 and other SCAs is not fully understood (Bezprozvanny and Klockgether, 2010; Kasumu and Bezprozvanny, 2012; Matilla-Dueñas et al., 2010).

PCs exhibit a tonic pacemaking activity that is crucial for the correct encoding of cortical cerebellar information to deep cerebellar nuclei and further to other motor coordination areas (Ito, 2002). In a recent study, we demonstrated that pacemaking activity of PCs is abnormal in aging SCA2 mice (Kasumu et al., 2012). Similar disruptions of PC pacemaking have been reported in slices from mouse models of SCA3 (Shakkottai et al., 2011) and episodic ataxia type-2 (EA2) (Walter et al., 2006). Small conductance Ca^{2+}-activated K^+ channels (SK channels) play a key role in the control of regular tonic firing in PCs (Womack and Khodakhah, 2003) and the two broad-specificity SK/IK channel activators chlorzoxazone (CHZ) and 1-ethyl-2-benzimidazolinone (1-EBIO) normalize PC firing and exert beneficial effects in a mouse model of EA2 (Alviña and Khodakhah, 2010a, 2010b; Walter et al., 2006). Three subtypes of SK channels are expressed in the brain (Adelman et al., 2012; Kuiper et al., 2012) with the SK2 isoform predominant in PCs (Cingolani et al., 2002; Hosy et al., 2011; Sailer et al., 2004). Thus, the SK2 channel subtype is the most attractive pharmacological target for treatment of cerebellar ataxia. Indeed, we here directly demonstrate that SK2 controls normal PC pacemaking. We also demonstrate that application of the SK/IK

Table 1. Potency and Selectivity of Positive Modulators of SK Channels

EC_{50} Values	SK1	SK2	SK3
Riluzole	ND	ND	16
CHZ	ND	960[a]	ND
1-EBIO	650	722	589
SKA-31	2.9[b]	1.9[b]	2.9[b]
CyPPA	>100[c]	14[c]	6[c]
NS309	0.6	0.8	0.9
NS13001	>10	1.8	0.14

ND, non-determined. All EC_{50} values indicated in μM. EC_{50} values for NS13001 are from the data summarized in Figure 3D. EC_{50} values for CyPPA are from (Hougaard et al., 2007). EC_{50} values for Riluzole, 1-EBIO, and NS309 are from in-house NeuroSearch data generated in a similar manner as those for NS13001 and CyPPA. Data on 1-EBIO and NS309 on SK2 is based on an extended data set compared to previously published data (Pedarzani et al., 2005). The data for other compounds are from the references as indicated.
[a]Cao et al. (2001).
[b]Sankaranarayanan et al. (2009).
[c]Hougaard et al. (2007). See also Figure S2.

modulator NS309 and the SK3/SK2 modulator CyPPA restore regular pacemaker activity of cerebellar PCs from SCA2 transgenic mice. We further report development of a more potent and selective modulator of SK2/3 channels (NS13001) and show that oral delivery of this compound resulted in significant beneficial effects in the transgenic mouse model of SCA2. We conclude that NS13001 holds promise as a potential therapeutic agent for treatment of SCA2 and possibly other cerebellar ataxias.

RESULTS

SK2 Channels Play a Key Role in Control of PCs Spontaneous Activity

SK channels play a key role in the control of pacemaking in PCs (Womack and Khodakhah, 2003). To confirm that positive SK modulators can exert a modulatory effect on PC firing, we performed a series of whole-cell recordings of PC activity in rat cerebellar slices using NS309 (3-oxime-6,7-dichloro-1H-indole-2,3-dione), a high potency positive modulator of SK/IK channels (Table 1) (Strøbaek et al., 2004). In the majority of experiments, regular action potential (AP) firing of PCs occurring in the frequency range 20–30 Hz (average frequency 23 ± 5 Hz [n = 6 PCs]) was recorded under control conditions resulting in an interspike interval close to 50 ms (Figures 1A and 1B). Bath application of 3 μM NS309 caused a marked reduction in the firing frequency to 9 ± 3 Hz (n = 6 PCs) (Figure 1A) and a concomitant increase in the interspike interval to above 150 ms (Figure 1B). The effect of NS309 was reversible and the spontaneous activity of PCs was restored toward the initial frequency following wash-out (Figure 1A). Prolonged exposure to NS309 frequently lead to a complete silencing of the cell (not shown) but upon extended wash-out, pacemaker activity could be restored. The bee venom toxin apamin specifically blocks SK channels (Adelman et al., 2012). Within minutes of application, 200 nM apamin changed the firing pattern of PCs from tonic to regular frequency bursts separated by silent periods (Figure 1A). The interspike interval within each burst was reduced to <15 ms in the presence of apamin (Figure 1B). Three subtypes of SK channels are expressed in the brain (Adelman et al., 2012; Patkó et al., 2003; Sailer et al., 2002, 2004). The SK2 isoform is highly expressed in PCs (Cingolani et al., 2002; Hosy et al., 2011; Sailer et al., 2004). In order to evaluate the importance of this subtype for regulating the intrinsic firing properties of PCs, we challenged regularly firing cells with the highly potent and selective synthetic SK2 toxin inhibitor Lei-Dab7 (Shakkottai et al., 2001). We confirmed the subtype specificity of the Lei-Dab7 batch available for this study (Figure S1 available online). In experiments with recombinant channels we demonstrated that Lei-Dab7 inhibits hSK2 channels with IC_{50} equal to 7 ± 1 nM (n = 3). In contrast, Lei-Dab7 inhibited recombinant hSK3 channels with IC_{50} equal to 1.8 ± 0.6 μM (n = 3) and recombinant hSK1 channels with IC_{50} equal to 27 ± 11 μM (n = 3). Thus, our batch of Lei-Dab7 is at least 200-fold more potent on SK2 channels when compared to SK1 and SK3 channels, in agreement with the published observations (Shakkottai et al., 2001). We discovered that at 100 nM, a concentration that strongly inhibits SK2 but does not affect SK1 or SK3 channels (Figure S1), Lei-Dab7, like apamin, changed the rat PC firing pattern from tonic into pronounced bursting (Figure 1C). The results with Lei-Dab7 support the key role of SK2 channels in control of PC pacemaking activity, in agreement with recently reached conclusions (Hosy et al., 2011).

SK2/3 Modulators Normalize Firing Activity of PCs from SCA2 Transgenic Mice

Previously, we discovered that cerebellar slices from aging SCA2-58Q (58Q) transgenic mice have a significantly higher fraction of bursting PCs when compared to slices from age-matched wild-type mice (Kasumu et al., 2012). Consistent with these findings, we found that most PCs (91 ± 10%) in slices from 24-week-old wild-type mice exhibited tonic activity (Figure 2A) characterized by stable firing rates (Figure 2C). In contrast, fewer PCs (64 ± 9%) in slices from 24-week-old 58Q mice exhibited tonic activity. PCs in slices from 24-week-old SCA2-58Q mice instead exhibited bursting activity (Figure 2B). We observed various firing patterns in bursting 58Q PCs. Some PCs fired regular high-frequency bursts separated by brief silent periods, a pattern that we named "persistent bursting" (Figures 2B and 2D). Other PCs displayed periods of relatively constant frequency firing separated by short periods of silence or increased frequency of firing. These cells were classified as "transiently bursting." In the previous study, we reasoned that the burst firing pattern of SCA2 PCs reflects the deteriorating health and loss of metabolic control of these cells and that this might be causally connected with the impaired motor performance of aging SCA2 mice (Kasumu et al., 2012). Thus, agents that can switch bursting SCA2 PCs to tonic firing may have a potential therapeutic value for SCA2.

To investigate if modulators of SK channels can rescue the abnormal firing of SCA2 PCs, we performed experiments with slices from 24-week-old 58Q mice in the presence of the pan-SK channel modulator NS309 and the selective SK2/3 modulator CyPPA (cyclohexyl-[2-(3,5-dimethyl-pyrazol-1-yl)-6-methyl-pyrimidin-4-yl]-amine) (Hougaard et al., 2007) (Table 1).

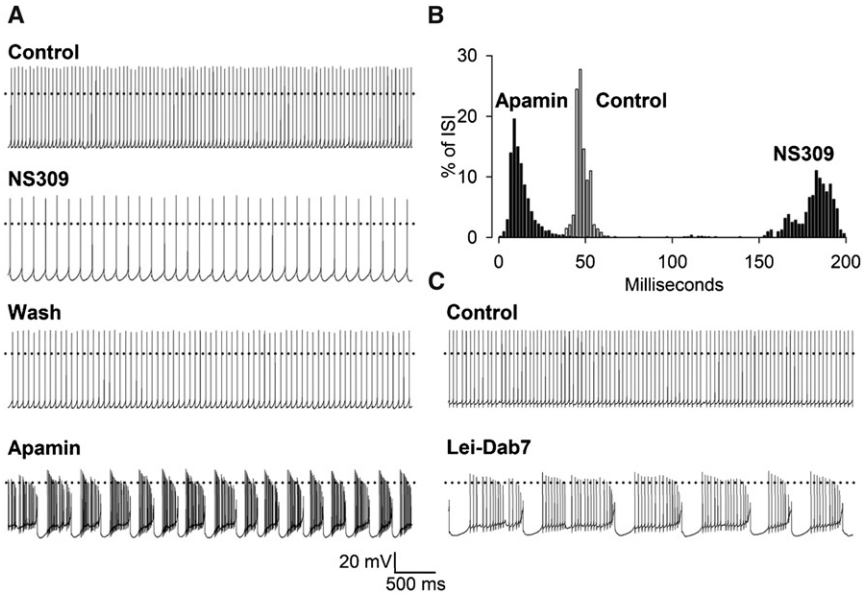

Figure 1. The Spontaneous Action Potential Firing of Rat Purkinje Neurons Is Sensitive to SK Channel Modulators

(A) Typical pacemaker-like spontaneous activity recorded under control conditions or in the presence of the positive modulator NS309 (3 μM) or the SK channel inhibitor apamin (200 nM).

(B) Histograms of interspike interval constructed from 1 min periods either in the absence of compound or following application of NS309 or apamin.

(C) Typical pacemaker-like spontaneous activity is reverted into burst firing by application of the SK2-selective SK channel inhibitor Lei-Dab7 (100 nM). Dotted lines indicate 0 mV.

See also Figure S1.

Application of 5 μM NS309 switched "persistently bursting" 58Q PCs to tonic firing pattern (Figure 2E; n = 11 of 11 PCs). Application of 5 μM NS309 also switched "transiently bursting" 58Q PCs to tonic firing pattern (Figure 2G; n = 7 of 7 PCs). CyPPA was less effective than NS309 in experiments with persistently bursting PCs because application of 5 μM CyPPA failed to switch persistently bursting 58Q PCs to tonic firing pattern in 6 out of 11 experiments (Figure 2F). However, similar to NS309, application of 5 μM CyPPA switched transiently bursting SCA2-58Q PCs to tonic firing pattern (Figure 2H; n = 6 of 7 PCs). These experiments suggested that activation of SK2 channels provides a potential strategy for restoring tonic firing of PC cells in aging SCA2 mice. When compared to NS309, the lower efficacy of CyPPA in these experiments is likely to be due to the relatively lower potency of this compound as an SK2 channel modulator (Hougaard et al., 2007) (see also Table 1).

NS13001 Is a More Selective and Potent Positive Modulator of SK2/3 Channels

The SK channel activators CHZ, 1-EBIO and SKA-31 used in previous studies with EA2 and SCA3 ataxic mice (Alviña and Khodakhah, 2010a, 2010b; Shakkottai et al., 2011; Walter et al., 2006) have low potency and lack subtype selectivity (Table 1). CyPPA (Figure 3A) is a well-characterized and selective positive modulator of SK2/3 channels (SK3 > SK2 >>> SK1 = IK) (Hougaard et al., 2007) (Table 1; Figure S2), whereas NS309 (Figure 3A) is the potent pan-selective IK/SK channel modulator (IK > SK1 = SK2 = SK3) (Strøbaek et al., 2004) (Table 1; Figure S2). In our studies we set out to develop an SK channel modulator that combines potency of NS309 and selectivity of CyPPA. To achieve this goal, a chemical optimization program based on the CyPPA scaffold was conducted at NeuroSearch (Palle Christophersen, personal communication), leading to the compound NS13001 (4-Chloro-phenyl)-[2-(3,5-dimethyl-pyrazol-1-yl)-9-methyl-9*H*-purin-6-yl]-amine) (Figure 3A) (Eriksen et al., 2008). The procedures for chemical synthesis of NS13001 (Figure S3) are described in the Supplemental Experimental Procedures. In experiments using inside-out patches, 1 μM NS13001 potently activated hSK3, less potently hSK2 and had no activating effect on hSK1 (Figure S2) or hIK channels (data not shown). Thus, NS13001 recapitulates the basic subtype selectivity properties of the lead molecule CyPPA, but with the potency comparable to NS309. When compared to NS309 and CyPPA, NS13001 also exerted less off-target effects. In the micromolar concentration range NS309 blocks hERG channels (IC_{50} = 1.3 μM) (Strøbaek et al., 2004) and CyPPA blocks voltage-gated sodium channels (IC_{50} = 11 μM) (Hougaard et al., 2007), whereas NS13001 had no effect on these channels at concentrations as high as 10 μM (data not shown).

NS13001 Is an Allosteric Modulator of SK2/3 Channels

The mechanism of NS13001 action was characterized in more detail, using hSK3 channels. Figure 3B shows current-voltage (I-V) relationships measured at symmetrical K^+ and with Ca^{2+} buffered at 0.2 μM Ca^{2+} or 10 μM Ca^{2+} (solid lines). Application of NS13001 in the range from 0.001 μM to 10 μM to the inside of the patch at a $[Ca^{2+}]_i$ of 0.2 μM resulted in a concentration-dependent increase in the hSK3 current (Figure 3B, broken lines). The maximal activation of hSK3 channels by NS13001 was 90% of the level observed at 10 μM cytosolic Ca^{2+} that activates SK channels maximally (Figure 3B). The characteristic inward rectification of the current was maintained when the channels were activated by NS13001 at low Ca^{2+} (Figure 3B). Figure 3C depicts the hSK3 current recorded at −75 mV as a function of time showing the effects of increasing concentrations of NS13001. To quantify the concentration-dependence of NS13001, a number of similar experiments were performed with patches from hSK1, hSK2, and hSK3 expressing cells and the current response in each experiment was normalized to the size of the current recorded at 10 μM Ca^{2+} for the same patch. The normalized data were averaged and plotted as a function of NS13001 concentration for each hSK subtype (Figure 3D). Data fitted by the Hill equation (solid line) yielded an EC_{50} value for hSK3 activation of 0.14 μM, a Hill coefficient of 1 and an efficacy of 91% (Figure 3D; Table 1). For hSK2 the EC_{50} was 1.6 μM, the Hill coefficient was 1.4 and the efficacy was

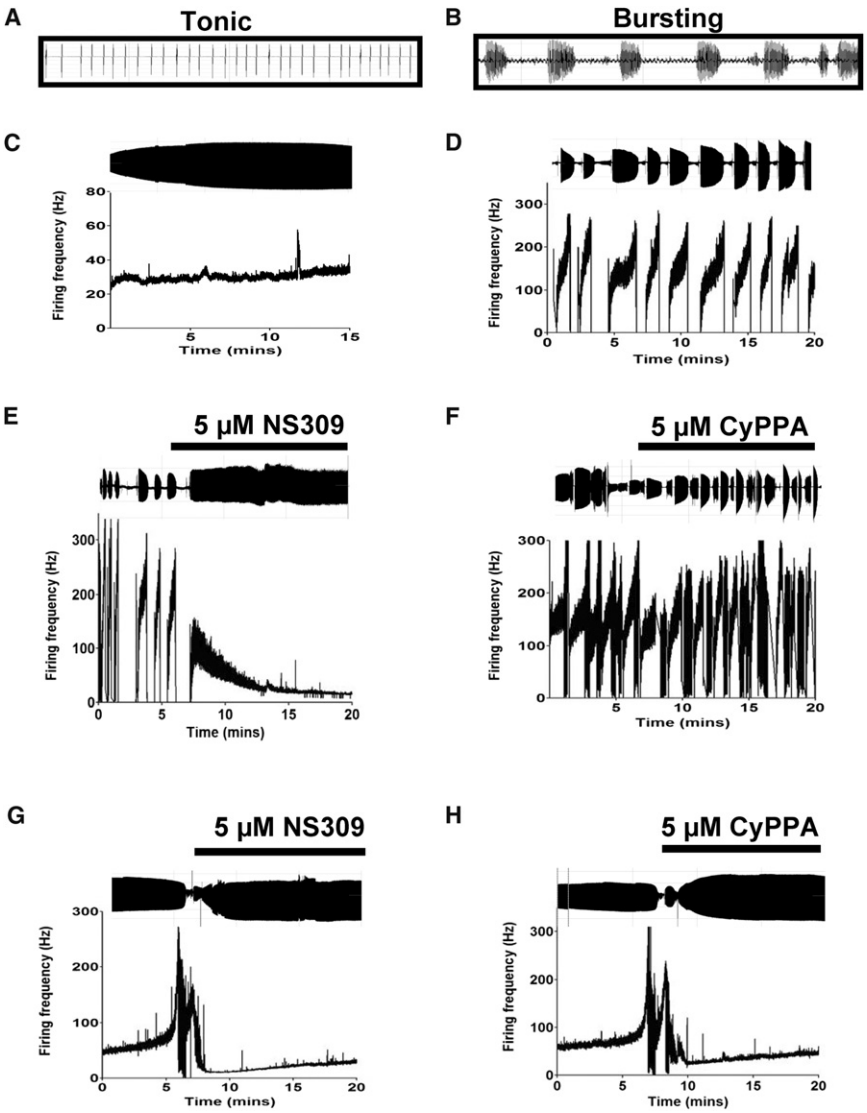

Figure 2. Positive Modulators of SK Channels Revert Bursting Firing of PC Cells from 24-Week-Old SCA2-58Q Mice

(A) Example of current records of tonically firing 58Q PCs (1 s trace).

(B) Example of current records of bursting 58Q PC (1 s trace).

(C) Example of the firing rate plot of tonically firing 58Q PC (15 min recording). The current record from the same cell is shown above the firing rate plot.

(D) Example of the firing rate plot of bursting 58Q PC (20 min recording). The current record from the same cell is shown above the firing rate plot.

(E) Application of 5 μM NS309 reverted "persistently bursting" 58Q PC to tonic firing pattern. The firing rate plot (20 min recording) and the current record for the same cell are shown. The time of 5 μM NS309 application is indicated by a bar.

(F) Application of 5 μM CyPPA often failed to revert "persistently bursting" 58Q PC to tonic firing pattern. The firing rate plot (20 min recording) and the current record for the same cell are shown. The time of 5 μM CyPPA application is indicated by a bar.

(G) Application of 5 μM NS309 reverted "transiently bursting" 58Q PC to tonic firing pattern. The firing rate plot (20 min recording) and the current record for the same cell are shown. The time of 5 μM NS309 application is indicated by a bar.

(H) Application of 5 μM CyPPA reverted "transiently bursting" 58Q PC to tonic firing pattern. The firing rate plot (20 min recording) and the current record for the same cell are shown. The time of 5 μM CyPPA application is indicated by a bar.

90% (Figure 3D; Table 1), whereas concentrations of NS13001 higher than 10 μM were needed to induce only a marginal increase in the hSK1 current (Figure 3D; Table 1). These results confirmed that the subtype selectivity properties of NS13001 is SK3 > SK2 >>> SK1.

To further understand the mechanism of NS13001 action, we evaluated the Ca^{2+}-dependence of its effects on SK channels. At very low cytosolic Ca^{2+} concentrations ($\leq$0.01 μM Ca^{2+}), the application of 1 μM NS13001 did not result in increased activity of hSK3 channels (Figures 3E and 3F). In contrast, in the middle range Ca^{2+} concentrations (0.2 μM Ca^{2+}), application of 1 μM NS13001 induced a large, reversible increase in the current level at all membrane potentials tested (Figures 3E and 3F). At high cytosolic Ca^{2+} concentration (10 μM Ca^{2+}), the application of NS13001 induced a small, but significant reduction in the hSK3 current level (Figures 3E and 3F). To test the effects on the SK Ca^{2+}-dependence more generally, we determined the Ca^{2+}-activation curves of hSK1, hSK2 and hSK3 in the absence or presence of 1 μM NS13001. In the absence of compound, the Ca^{2+}-dependence for all 3 SK channel subtypes is virtually identical, with EC_{50} of 0.42 μM Ca^{2+} (Hougaard et al., 2007) (Figure 3G, dashed line). The presence of 1 μM NS13001 induced a pronounced left-ward shift in the Ca^{2+}-activation curve of hSK3, resulting in an EC_{50} for Ca^{2+} of 0.11 μM (Figure 3G). Presence of NS13001 also resulted in a small reduction in the maximal activity of hSK3 channels at the highest Ca^{2+} concentrations (Figure 3G). Similarly, 1 μM NS13001 also increased the apparent Ca^{2+}-sensitivity of hSK2, with a new EC_{50} = 0.18 μM (Figure 3G) and induced a small reduction of the hSK2-mediated current at high Ca^{2+} concentrations (Figure 3G). In contrast to hSK2 and hSK3 channels, 1 μM NS13001 did not have any stimulating effect on the Ca^{2+} dependence of hSK1 channels, but also resulted in a reduction of the current at high concentrations of Ca^{2+} (Figure 3G). Based on the obtained results, we conclude that NS13001 primarily acts as a potent and selective positive allosteric modulator of SK2 and SK3 channels.

Oral Treatment of SCA2 Mice with SK2/3 Positive Modulators Improves Motor Performance

In order to test the effects of SK channel positive modulators on the motor performance of symptomatic SCA2 mice, we

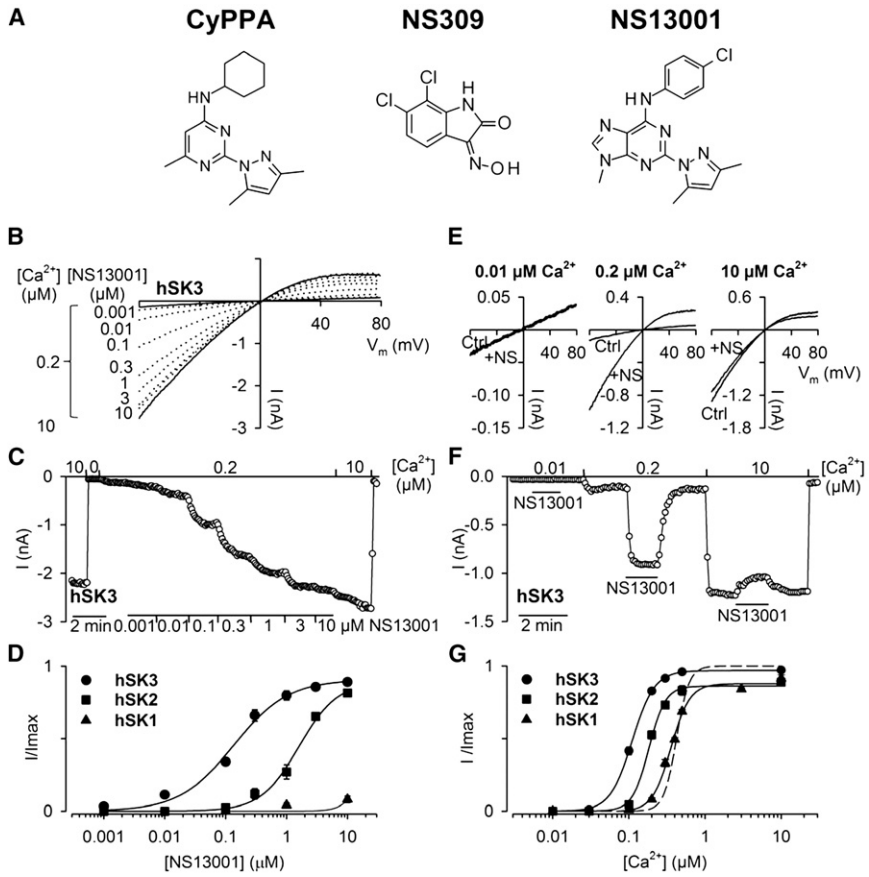

Figure 3. NS13001 Is a More Selective Allosteric Modulator of SK3 and SK2 Channels

(A) Chemical structures of CyPPA, NS309, and NS13001.

(B) Current-voltage (I-V) relationships measured in i-o patches from HEK293 cells expressing hSK3. Currents recorded at 0.2 μM Ca^{2+} and 10 μM Ca^{2+} are shown by solid black lines. The currents recorded at 0.2 μM Ca^{2+} in the presence of increasing concentrations of NS13001 (indicated in μM) are shown by dotted lines.

(C) hSK3 current at −75 mV obtained from the voltage ramps (as in B) plotted as a function of time. The patch was exposed to a cytosolic Ca^{2+} of 0.01 μM, 0.2 μM or 10 μM as indicated. At 0.2 μM Ca^{2+}, NS13001 was applied at the concentrations indicated (in μM).

(D) Concentration-dependence of SK channel activation by NS13001. The currents were measured in i-o patches at 0.2 μM Ca^{2+}. The currents at each NS13001 concentration were normalized to the current in the same patch at 10 μM Ca^{2+}, averaged and shown at each NS13001 concentration as mean ± SE ($n \geq 3$ experiments) for hSK1 (triangles), hSK2 (squares), and hSK3 (circles) expressing cells. The solid lines are the fit of the data to the Hill equation (hSK3: EC_{50} = 0.14 μM, n_H = 1.0; hSK2: EC_{50} = 1.8 μM and n_H = 1.4; hSK1: EC_{50} > 100 μM).

(E) I-V relationships at a cytosolic Ca^{2+} concentration of 0.01 μM, 0.2 μM, or 10 μM in the absence (Ctrl,) or presence (+NS) of 1 μM NS13001.

(F) hSK3 current at −75 mV plotted as a function of time. The patch was exposed to a cytosolic Ca^{2+} of 0.01 μM, 0.2 μM or 10 μM as indicated. The times of 1 μM NS13001 application are shown by bars.

(G) Ca^{2+}-dependence of hSK channels in the presence of 1 μM NS13001. Ca^{2+}-sensitivity of all three SK subtypes is identical in the absence of the compounds (dashed line, EC_{50} = 0.42 μM Ca^{2+}, n_H = 5.2). In the presence of 1 μM NS13001 the averaged data at each cytosolic Ca^{2+} concentration are shown as mean ± SE ($n \geq 3$ experiments) for patches from hSK1 (triangles), hSK2 (squares), and hSK3 (circles) expressing cells. The solid lines are the fit of data to the Hill equation (hSK3: EC_{50} = 0.11 μM Ca^{2+}, n_H = 3.0; hSK2: EC_{50} = 0.18 μM Ca^{2+} and n_H = 4.0; hSK1: EC_{50} = 0.36 μM Ca^{2+} and n_H = 3.5).

See also Figure S3.

evaluated the effects of oral delivery of NS13001 and CyPPA to a group of 9-month-old 58Q mice. NS309 was not utilized in these studies as our pilot studies demonstrated that this compound is less stable in vivo and has significantly inferior pharmacokinetic and brain penetration properties compared to NS13001 and CyPPA (data not shown). Thus, although NS309 provides a powerful tool for in vitro experiments with brain slices (Figures 1 and 2), it is less appropriate for in vivo long term studies with repeated dosing. The in vivo studies were designed following the same general principles as in the previous evaluation of dantrolene feeding and 5PP overexpression in 58Q mice (Kasumu et al., 2012; Liu et al., 2009). Briefly, 9-month-old WT and 58Q mice were subdivided into six treatment groups with 10–15 mice in each group (Table 2). We confirmed that the average weight of the mice was similar for each group (Figure S4). The baseline motor performance was evaluated by beamwalk (11 mm round and 5 mm square beams) and accelerating rotarod assays. Consistent with the previous results (Kasumu et al., 2012; Liu et al., 2009), 9-month-old 58Q mice were impaired in both assays when compared to age-matched wild-type mice (Figures 4 and S5). Following the baseline test, the mice were orally fed daily with 30 mg/kg NS13001 or 10 mg/kg CyPPA. The dose of CyPPA was chosen based on the previous in vivo studies with this compound (Herrik et al., 2012; Vick et al., 2010). The higher dose of NS13001 was chosen based on its more favorable target selectivity profile. In pilot experiments, we established that 1 hr after oral delivery of 30 mg/kg of NS13001 to adult mice the concentration in blood plasma was 16 μM (8 μM after 6 hr). After 1 hr, the concentration in the brain was 17 μM (data not shown).

The 58Q and WT mice were fed with the compound orally starting at 9 months of age for 3 consecutive weeks with the control mice fed with the vehicle alone. After 3 weeks on this dosing regimen, feeding of the compounds was halted for 3 days. Following this brief washout period, motor coordination of each mouse was retested using identical beamwalk and rotarod assays. The average body weight for all six groups remained constant after feeding with the compounds (Figure S4). All three groups of WT mice displayed similar levels of motor performance after drug treatment. The latency of crossing the 11 mm beam was reduced for all three groups of WT mice (Figure 4A), presumably due to learning the task. There was no

Table 2. Evaluation of NS13001 and CyPPA in SCA2 Mouse Model

				DCD Measurements			
Group	Gen	Compound	No. of Animals	No. of PCs Counted	Normal (%)	Moderate (%)	Severe (%)
1	WT	Vehicle	10 (7)	258	72 ± 6	22 ± 3	7 ± 3
2	WT	CyPPA	13 (9)	245	84 ± 3	10 ± 2	6 ± 2
3	WT	NS13001	10 (7)	255	82 ± 8	11 ± 4	7 ± 5
4	58Q	Vehicle	15 (11)	296	12 ± 3	51 ± 11	38 ± 10
5	58Q	CyPPA	14 (10)	222	33 ± 5*	35 ± 6	33 ± 11
6	58Q	NS13001	20 (16)	288	43 ± 5*	38 ± 7	19 ± 4

DCD, dark cell degeneration; PC, Purkinje cells. The number of mice in each group in the beginning of drug feeding is shown. The number of mice which survived until the end of the study is shown in parentheses. Two-tailed Student's unpaired t test was used to judge differences between compound-treated groups and the placebo groups.
*$p < 0.001$. See also Figure S4.

difference in the number of foot slips that mice made crossing the 11 mm beam (Figure 4B). Testing on the 5 mm square beam revealed that the latency to cross and the number of foot slips remained the same for all three groups of mice (Figure S5).

The control (vehicle-fed) group of 58Q mice traversed the 11 mm and 5 mm beams posttreatment similarly as prior to treatment (Figures 4A and S5) and there was no significant difference in the number of foot slips (Figures 4B and S5). The rotarod performance of the vehicle-fed group of 58Q mice remained the same as prior to treatment (Figure 4C). In contrast to WT mice, NS13001-fed 58Q mice demonstrated significantly improved performance following treatment with the compound. In the 11 mm beam task a decrease in the latency to traverse the beam (Figure 4A; $p < 0.01$) and a decreased number of foot slips (Figure 4B; $p < 0.05$) were observed. Both effects were replicated on the 5 mm beam (Figure S5). There was also a significant increase in the latency to fall off the accelerating rod following feeding of 58Q mice with NS13001 (Figure 4C; $p < 0.05$). Treatment with CyPPA also resulted in improved motor performance of 58Q mice, although beneficial effects were less pronounced than for NS13001. Treatment of 58Q mice with CyPPA resulted in a reduced latency ($p < 0.05$) to cross the 11 mm and 5 mm beams (Figures 4A and S5) but had no significant effect on the number of foot slips on either beam (Figure 4B; Figure S5) or on the rotarod performance of these mice (Figure 4C). The lower efficacy of CyPPA in these assays is probably explained by its lower potency (Table 1) and lower dosing level in the in vivo experiments. Following initial evaluation (Figures 4 and S5), we attempted to determine if effects of the drugs were reversible. All mice were returned to the home cages and retested again 2 months later. However, at this time-point the mice were 13 months old and many 58Q and WT had difficulty completing the motor tasks due to inability to remain on the balance beam or the rotating rod. For this reason we could not clearly discern treatment reversibility from other effects in this study.

Oral Treatment of SCA2 Mice with SK2/3 Positive Modulators Alleviates Brain Pathology

At 13 months of age (2 months after drug treatment was finished), all mice were sacrificed and processed for neuropathological analysis. In previous studies, we demonstrated that quantification of dark cell degeneration (DCD) provides the most reliable and most sensitive way to score excitotoxic PC death in 58Q mice (Kasumu and Bezprozvanny, 2012; Kasumu et al., 2012). DCD has also been used to quantify excitotoxic PC death in SCA7 and SCA28 (Custer et al., 2006; Maltecca et al., 2009). DCD is a form of PC death characterized by morphological changes in PCs identifiable by transmission electron microscopy (TEM) of slices from 58Q mice (Figure 5A, right panel). In contrast, most PCs in age-matched WT mice look normal (Figure 5A, left panel). To analyze DCD, cerebellar sections from each of the six experimental groups of mice (Table 2) were processed for TEM and the number of normal, moderately, and severely degenerated PCs was quantified. According to (Kasumu and Bezprozvanny, 2012; Kasumu et al., 2012), PCs spherical in shape and with regular alignment in the PC layer were classified as "normal" (Figure 5B, left panel). PCs with slight shrinkage compared to surrounding PCs and with moderately electron-dense cytosol that is not as dark as the nucleus, were classified as "moderate" (Figure 5B, middle panel). PCs with markedly shrunken and electron-dense cytosol with similarly darkened nucleus were classified as "severe" (Figure 5C, right panel). Consistent with our previous data (Kasumu and Bezprozvanny, 2012; Kasumu et al., 2012), we found that in samples from 58Q control mice, 12% of PCs were normal, 51% were moderately degenerated, and 38% were severely degenerated (n = 296 PCs; Figure 5C; Table 2). Also consistent with our previous data (Kasumu and Bezprozvanny, 2012; Kasumu et al., 2012), most cells were healthy in samples from age-matched WT control mice, in which 72% of PCs were scored as normal, 22% were moderately degenerated and 7% were severely degenerated (n = 258 PCs; Figure 5C; Table 2). The WT mice treated with NS13001 or CyPPA did not exhibit a significant change in the number of normal cells and moderately affected cells (Figure 5C; Table 2). In contrast, in the samples from the 58Q mice exposed to NS13001, the fraction of normal PCs was increased to 43%, moderately degenerated cells reduced to 38% and degenerated cells reduced to 19% (n = 288 PCs; Figure 5C; Table 2). Similarly, in samples from CyPPA-treated 58Q mice the fraction of normal cells was increased to 33%, the fractions of moderately degenerated cells and severely degenerated cells were reduced to 35% and 33%, respectively (n = 222 PCs; Figure 5C; Table 2). When compared to vehicle-treated 58Q mice, the increase in the fraction of normal cells in 58Q mice treated with NS13001 or CyPPA was

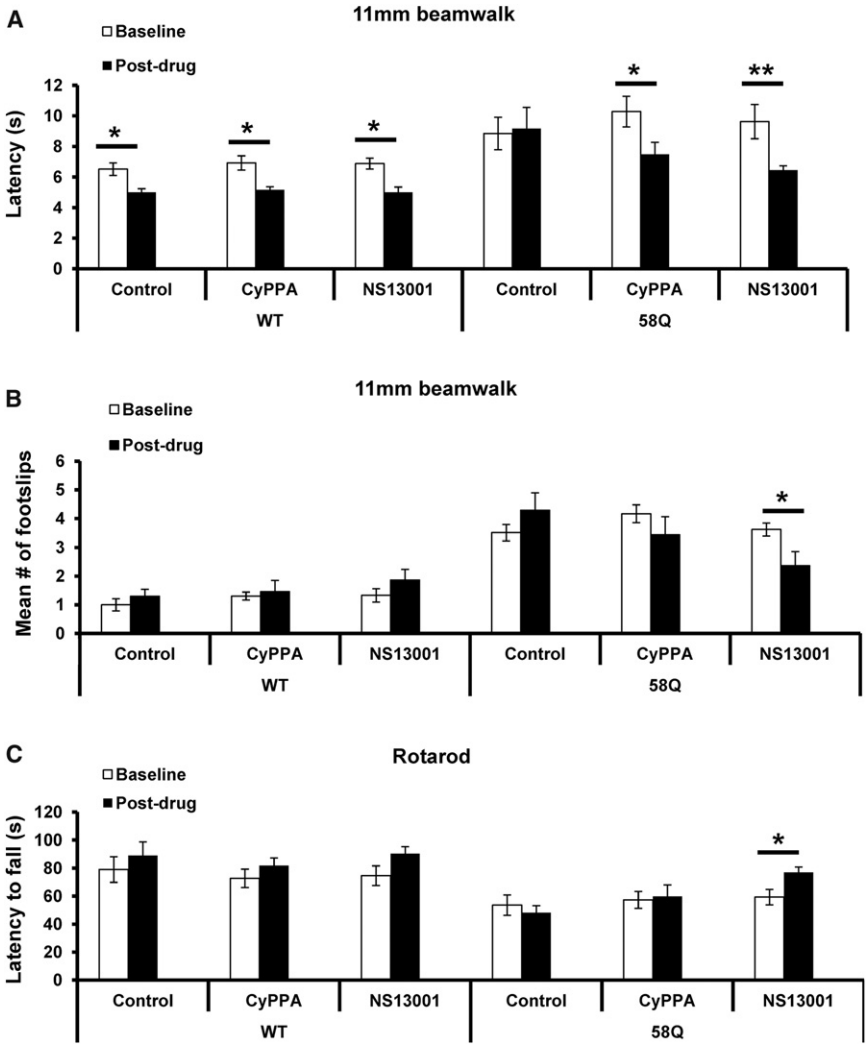

Figure 4. Oral Treatment of Aging SCA2 Mice with SK2/3 Channel Positive Modulators Improves Motor Performance

(A and B) At baseline, after drug treatment, mice from all six groups were trained on the 17 mm, 11 mm, and 5 mm beams. Average time to traverse the entire length of each beam is recorded. Mean latency to traverse 11 mm beams before (white bars) and after (black bars) 3 weeks of chronic drug treatment is plotted for each group of mice as mean ± SE. The WT control mice (WT), WT mice fed with CyPPA (WT-CyPPA), WT mice fed with NS13001 (WT-NS13001), 58Q control mice (58Q), the 58Q mice fed with CyPPA (58Q-CyPPA), and the 58Q mice fed with NS13001 (58Q-NS13001) (A). Average number of foot slips as the mice traverse the entire length of the 11 mm beam was also recorded. Mean number of foot slips as the mice traverse the 11 mm beams before (white bars) and after (black bars) 3 weeks of chronic drug treatment is also plotted for each group of mice (B).

(C) Mice were trained on the accelerating rotarod. Mean latency to fall off rotarod before (white bars) and after (black bars) 3 weeks of chronic drug treatment is plotted for each group of mice as mean ± SE. *$p < 0.05$; **$p < 0.01$ when compared to baseline performance.

See also Figure S5.

statistically significant ($p < 0.001$; Figure 5C; Table 2). Similar to behavioral studies (Figures 4 and S5), the beneficial effects of CyPPA in DCD assay with 58Q mice were less pronounced than the beneficial effects of NS13001 in the same assay (Figure 5C; Table 2).

DISCUSSION

SK2 Channels as Targets for Treatment of Cerebellar Ataxia

The cerebellum plays an essential role in learning and control of coordinated movements. The precision and speed of these movements requires exact timing of cerebellar output. The inhibitory projections from the PC to the deep cerebellar nuclei (DCN) constitute the sole output of the cerebellar cortex (Ito, 2002). Recent electrophysiological analysis confirmed that PC electrical activity is tightly coordinated at millisecond resolution (de Solages et al., 2008; Heck et al., 2007; Person and Raman, 2012). In slices, PCs spontaneously fire action potentials at a constant frequency in the range 17–150 Hz (Llinás and Sugimori, 1980a, 1980b; Nam and Hockberger, 1997; Raman and Bean, 1997, 1999; Smith and Otis, 2003; Womack and Khodakhah, 2002). It is generally believed that this endogenous pacemaking activity of PCs represents the crucial background activity for correct encoding of the integrated cerebellar cortex information to DCN and other motor coordination areas. Cerebellar PCs are affected in many ataxias (Carlson et al., 2009; Matilla-Dueñas et al., 2010; Orr and Zoghbi, 2007), and massive PC death is observed at the end stage of disease for many ataxic patients. However, it is becoming evident that early symptoms of ataxia may result not from PCs death but from PCs dysfunction and loss of firing precision. Consistent with this hypothesis, disruptions of regular PCs pacemaking activity have been uncovered in studies with mouse models of EA2 (Walter et al., 2006), SCA3 (Shakkottai et al., 2011), and SCA2 (Kasumu et al., 2012). Based on these findings, it has been argued that drugs that can normalize the regular firing of PCs may provide therapeutic benefit for ataxic patients (Rinaldo and Hansel, 2010; Shakkottai et al., 2004, 2011; Walter et al., 2006).

There are multiple ion conductances that control the spontaneous electrical activity of PCs (Llinás and Sugimori, 1980a, 1980b; Raman and Bean, 1997, 1999). Small conductance Ca^{2+}-activated K^+ channels (SK channels) emerged as one of the principle channel types involved in precise control of PC pacemaking (Womack and Khodakhah, 2003). A number of small molecule modulators of SK channels have previously been identified (Table 1), enabling pharmacological manipulation of SK channel activity in ataxic mouse models. The two

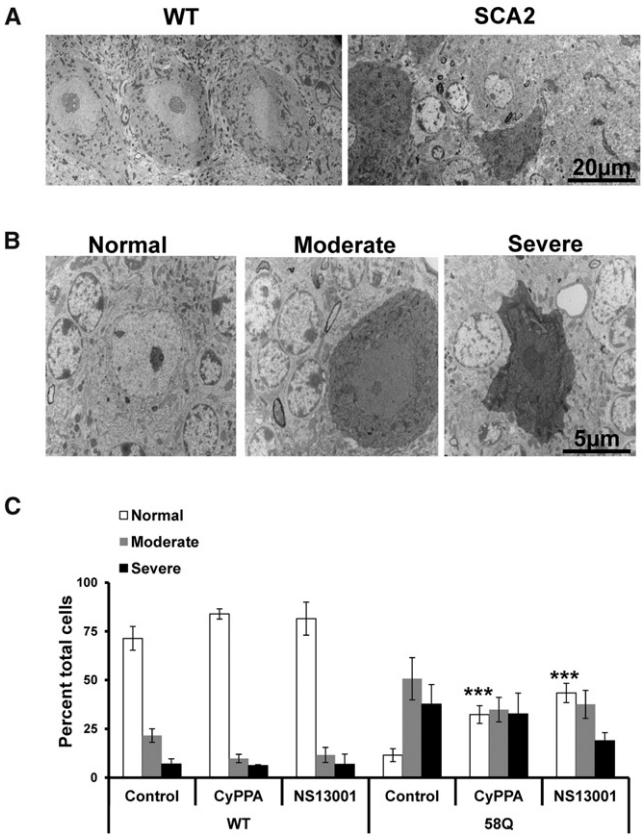

Figure 5. Oral Treatment of Aging SCA2 Mice with SK2/3 Channels Positive Modulators Improves SCA2 Pathology

(A and B) Examples of normal and affected PCs from WT and SCA2 mice as revealed by DCD staining protocol.

(C) Average percentage of normal, moderate and severely degenerated PCs in each group is plotted as mean ± SE. The chronic treatment of 58Q mice with NS13001 or CyPPA improved the DCD status of PCs when compared to vehicle treated 58Q mice (n = 222-296 PCs counted; ***$p < 0.001$).

broad-specificity SK/IK channel activators chlorzoxazone (CHZ) and 1-ethyl-2-benzimidazolinone (1-EBIO) normalized PC firing and exerted beneficial effects in a mouse model of EA2 (Alviña and Khodakhah, 2010a, 2010b; Walter et al., 2006). Short-term exposure of SCA3 mice to SKA-31, a riluzole analog optimized for positive modulation of SK channels (Table 1), provided benefit in a mouse model of SCA3 (Shakkottai et al., 2011). These results supported the hypothesis that positive modulators of SK channels may offer therapeutic benefit for treatment of ataxia. Indeed, riluzole yielded promising results in a recent phase II study in a mixed population of ataxia patients (Ristori et al., 2010), an effect that was interpreted as the ability of riluzole to facilitate the activity of SK channels (Table 1). Despite these promising results, most agents used in previous studies of ataxia had low potency, poor specificity and suboptimal blood brain permeability properties (Table 1).

Three subtypes of SK channels are expressed in the brain (Adelman et al., 2012; Kuiper et al., 2012; Patkó et al., 2003; Sailer et al., 2002; Stocker, 2004; Stocker and Pedarzani, 2000). The SK2 isoform is predominant in PCs (Cingolani et al., 2002; Hosy et al., 2011; Sailer et al., 2004), whereas high levels of SK3 channels are expressed in cerebellar granule cells (Stocker and Pedarzani, 2000). SK3 single knockout mice lack a clear motor phenotype (Bond et al., 2000), but showed increased dopamine release in the striatum and certain changes in models of depression and anxiety (Jacobsen et al., 2009, 2008). A naturally occurring SK2 loss-of-function mutation in mice (*frissonant* mice) causes prominent motor deficits (Callizot et al., 2001). In experiments with the SK2-specific synthetic toxin inhibitor Lei-Dab7 (Shakkottai et al., 2001) we now demonstrate the essential role of SK2 channels in the control of PCs spontaneous activity (Figure 1C). These results are in agreement with a recent report (Hosy et al., 2011). Furthermore, we demonstrated that the potent pan-SK channel modulator NS309 converted the "burst" firing pattern of aging PC cells from SCA2 transgenic mouse model to a tonic firing pattern (Figures 2E and 2G). The SK2/3-selective modulator CyPPA was also able to restore the "tonic" firing pattern of some SCA2-PCs but appeared less effective (Figures 2F and 2H). The difference between the effect of NS309 and CyPPA is most likely due to the substantially lower potency of CyPPA in activating SK2 channels (Table 1; Figure S2). Based on all these results we concluded that the SK2 channel subtype is the most attractive pharmacological target for treatment of cerebellar ataxia. We therefore set out to develop a more selective and potent SK2/3 positive modulator with CyPPA as lead molecule with improved pharmacokinetic and brain penetration properties.

NS13001 as a Potential Therapeutic Agent for Treatment of Cerebellar Ataxias

NS13001 is a molecule (Figure 3A) (Eriksen et al., 2008) identified in an optimization program based on CyPPA (Palle Christophersen, personal communication). Our electrophysiological experiments revealed that NS13001 recapitulates the basic subtype selectivity properties of the lead molecule CyPPA (hSK3 > hSK2>>>hSK1), with a potency comparable to NS309 (Figures 3 and S1; Table 1). Similar to CyPPA (Hougaard et al., 2007), NS13001 acts as an allosteric modulator of SK2/3 channels, which increases their sensitivity to activation by cytosolic Ca^{2+} (Figure 3G). NS13001 most likely binds in the binding pocket formed at the interface between calmodulin and SK2/3 channels, as has been recently suggested for CyPPA and NS309 based on crystallographic analysis (Zhang et al., 2012). When compared to CyPPA or NS309, NS13001 is considerably more stable toward metabolic degradation by liver microsomes in vitro (data not shown) and achieves significantly higher plasma and brain concentrations following oral administration to rats (data not shown). In our experiments, we evaluated a potential efficacy of N13001 and CyPPA in a transgenic mouse model of SCA2. In this mouse model human Atxn-58Q transgene is expressed under control of a PC-specific promoter (Huynh et al., 2000), resulting in progressive development of motor symptoms and loss of PCs (Huynh et al., 2000; Kasumu and Bezprozvanny, 2012; Liu et al., 2009; Kasumu et al., 2012).

Both NS13001 (30 mg/kg) and CyPPA (10 mg/kg) were fed to SCA2 mice for 3 consecutive weeks starting at 9 months of age. The dose of CyPPA utilized in these studies was chosen based on the previous in vivo studies with this compound (Herrik

et al., 2012; Vick et al., 2010) and its potential off-target effects (Hougaard et al., 2007). The higher dose of NS13001 was chosen based on its more favorable target selectivity profile. Following drug treatment, these mice were evaluated in motor coordination assays (balance beam walk and accelerating rotarod). We discovered that both NS13001 and CyPPA significantly improved performance of SCA2 mice in beamwalk assays, although effects of NS13001 were more pronounced (Figures 4A, 4B, and S5). The effects were specific, as performance of age-matched wild-type mice was not significantly affected by either compound (Figures 4 and S5). NS13001, but not CyPPA, demonstrated efficacy in the rotarod assay (Figure 4C). Overall, these data strongly indicated that oral exposure to positive modulators of SK2/3 channels have the potential of improving motor performance of aging SCA2 mice. Much to our surprise, the benefit of administering NS13001 and CyPPA to SCA2 mice extended beyond improved motor performance after 3 weeks. At the conclusion of the study, we evaluated excitotoxic PC death in 13 months old SCA2 mice by quantifying their dark cell degeneration (DCD) status (Kasumu and Bezprozvanny, 2012; Kasumu et al., 2012). We found that PCs in SCA2 mice were partially protected from DCD (Figure 5C; Table 2) by both NS13001 and CyPPA. Similar to the behavioral assays, the degree of protection appeared to be greater in NS13001-fed mice than in CyPPA-fed mice (Figure 5C; Table 2).

What is an explanation of these findings? And what is the physiological target of NS13001 and CyPPA in these experiments? Both compounds have significantly higher selectivity for SK3 than for SK2 (Table 1; Figures 3D and S1). However, in contrast to SK2, SK3 channels are not prominently expressed in PCs and the most likely molecular target of these compounds are thus SK2 channels (Cingolani et al., 2002; Hosy et al., 2011; Sailer et al., 2002, 2004). High levels of SK3 channels are expressed in cerebellar granule cells (Sailer et al., 2002, 2004; Stocker and Pedarzani, 2000) and in dopaminergic neurons of the substantia nigra (Sailer et al., 2002, 2004). In addition, both SK3 and SK2 channels are present in DCN (Sailer et al., 2004; Shakkottai et al., 2004; Stocker and Pedarzani, 2000). It cannot be excluded that some of the behavioral effects of NS13001 and CyPPA are due to activation of SK3 channels in non-PC neurons. However, as SK3 single knockout mice lack a clear motor phenotype (Bond et al., 2000), this is not very likely. Thus, we propose that the beneficial effects of NS13001 and CyPPA in the SCA2 mouse model are primarily due to ability of these compounds to potentiate activity of SK2 channels in PCs of aging SCA2 mice.

There are also several potential explanations for the observed beneficial effects. The first explanation is that NS13001 and CyPPA converted "bursting" to "tonic" pattern of PCs in aging SCA2 mice (Figure 2) and helped information processing in cerebellum of these mice by restoring regular firing of PCs. The second explanation is that NS13001 or CyPPA induced low frequency tonic firing pattern of all PCs in aging SCA2 mice. PC action potentials are coupled to increases in the intracellular Ca^{2+} concentration in PC soma and dendrites due to opening of P-type voltage-gated Ca^{2+} channels (Sabatini et al., 2001). Handling of this Ca^{2+}-influx puts PCs in conditions of latent metabolic stress, being proportional to the frequency of spontaneous firing, and likely to be strongly amplified during periods of uncontrolled bursting. Decreased frequency of PCs tonic firing and in particular reversion of bursting in the presence of NS13001 or CyPPA most likely reduces Ca^{2+} influx and leads to much lower metabolic demand of these cells. The reduction of Ca^{2+} influx is particularly critical for PCs in SCA2 mice, which already have supranomal cytosolic Ca^{2+} signals due to pathogenic interactions between mutant ataxin-2 and $InsP_3R1$ (Kasumu and Bezprozvanny, 2012; Liu et al., 2009; Kasumu et al., 2012). It is possible that during the drug administration period PCs in SCA2 mice were exposed to a 3-week "metabolic holiday," giving them a chance to recover from Ca^{2+} overload and rejuvenate. This latter explanation is consistent with DCD data collected 2 months after drug feeding was discontinued (Figure 5C; Table 2), which demonstrated long lasting neuroprotection in drug-exposed SCA2 mice. These results lead us to suggest that NS13001 and related compounds may exert not only symptomatic but also neuroprotective effects for cerebellar ataxia patients.

The proposed explanation of NS13001 or CyPPA ability to protect PCs in SCA2 mice is consistent with studies in Parkinson's disease (PD) field, where it was demonstrated that reducing voltage-dependent Ca^{2+} influx during pacemaker firing of substantia nigra (SNc) neurons leads to neuroprotection in models of PD (Chan et al., 2009, 2010; Surmeier, 2007; Surmeier et al., 2010) and possibly in PD patients (Becker et al., 2008; Ritz et al., 2010) (but see Louis et al., 2009; Simon et al., 2010). In case of studies in PD models, the Ca^{2+} influx in SNc neurons was reduced not by slowing down pacemaking activity of these cells but by pharmacological block of $Ca_V1.3$ voltage-gated Ca^{2+} channels which mediate most of Ca^{2+} influx in these cells during spontaneous activity (Chan et al., 2010). Similar to PCs, SK channels are involved in the control of firing rates of dopaminergic neurons in the SN neurons (Johnson and Wu, 2004; Kuznetsov et al., 2006; Shepard and Bunney, 1988), which express high levels of SK3 channels (Sailer et al., 2002, 2004). Downregulation of SK channels and increased bursting frequency of SN neurons have been related to PD-linked genetic mutations (Bishop et al., 2010). If NS13001 indeed acted in our experiments by reducing "metabolic burden" on SCA2 PC cells, it is likely that NS13001 and related compounds may offer potential benefit not only for cerebellar ataxias but also for PD and for other neurodegenerative disorders that affect SK2 or SK3-expressing pacemaking neurons. This hypothesis is consistent with recently reported neuroprotective effects of CyPPA in experiments with dopaminergic neuronal cultures (Benítez et al., 2011; Herrik et al., 2012) and with the recent mathematical simulations (Drion et al., 2012). The data in the current manuscript suggest that NS13001 should exert even more potent protective effect than CyPPA on SNc neurons both in vitro and in vivo. Evaluation of NS13001 in animal models of PD and other neurodegenerative disorders will be required to test these predictions.

The most serious potential side effects related to using modulators of SK2/3 channels are likely to be related to potential memory and learning impairments (Kuiper et al., 2012). Hippocampal-dependent memory tasks were potentiated by blocking SK channels with apamin (Stackman et al., 2002; Vick et al., 2010) and impaired by transgenic overexpression of SK2

channels (Hammond et al., 2006; Stackman et al., 2008). Transient downregulation of SK2 and SK3 channels was reported during spatial learning paradigm in rats (Mpari et al., 2010). Moreover, systemic administration of 15 mg/kg of CyPPA resulted in object memory encoding deficits in mice (Vick et al., 2010). Based on these results it is likely that the "therapeutic window" for usage of NS13001 and other SK2/3 modulators for treatment of neurodegeneration will be eventually determined by the balance between neuroprotective effects on bursting cells (such as PC cells in ataxias, SNc cells in PD) and memory impairing effects in hippocampus. Future studies with animal models of disease and human clinical trials will be needed to find an appropriate dosage and delivery regiment for these compounds to achieve maximal benefit with minimal side-effects.

SIGNIFICANCE

Cerebellar ataxias are a group of genetic disorders that are caused by progressive dysfunction and death of cerebellar PCs. SK channels play a key role in control of PC firing rates (Womack and Khodakhah, 2003) and a number of previous studies suggested that pharmacological modulators of SK channels may exert beneficial effects in cerebellar ataxia mouse models (Alviña and Khodakhah, 2010a, 2010b; Shakkottai et al., 2011; Walter et al., 2006). Riluzole yielded promising results in a recent phase II study in a mixed population of ataxia patients (Ristori et al., 2010), an effect that was suggested to be related to the ability of riluzole to facilitate the activity of SK channels. Despite these promising results, most agents used in previous studies of ataxia had low potency and poor specificity (Table 1). We report the development of a compound NS13001 that acts as a more potent and selective positive modulator of SK2/3 channels. We demonstrate that SK2 channels play a key role in control of pacemaking activity of cerebellar PCs and established that application of SK modulators restores tonic firing pattern of bursting PCs from aging mouse model of SCA2. We demonstrated that 3 weeks oral feeding of NS13001 resulted in improved performance of aging SCA2 mice in motor coordination assays and reduced PC degeneration in these mice. Similar, but less pronounced, positive effects were observed in SCA2 mice fed with CyPPA. The most likely mechanism responsible for beneficial effects of NS13001 and CyPPA is a reduction in Ca^{2+} influx and related metabolic stress due to normalized spontaneous activity of SCA2 PCs. From these results we conclude that NS13001 holds promise as a potential therapeutic agent for treatment of SCA2 and possibly other cerebellar ataxias. We reasoned that NS13001 may also be useful for treatment of other neurodegenerative disorders that affect pacemaking cells expressing SK2/3 channels, such as for example dopaminergic neurons in SNc (Benítez et al., 2011; Chan et al., 2009, 2010; Surmeier, 2007; Surmeier et al., 2010; Drion et al., 2012). Evaluation of NS13001 in animal models of ataxia, PD, and other neurodegenerative disorders will be required to test these predictions. The most serious potential side effects related to using modulators of SK2/3 channels are likely to be related to potential memory and learning impairments (Hammond et al., 2006; Stackman et al., 2008; Vick et al., 2010), which may eventually determine a limit on clinically useful doses of these compounds for treatment of neurodegeneration.

EXPERIMENTAL PROCEDURES

Compounds

Cyclohexyl-[2-(3,5-dimethyl-pyrazol-1-yl)-6-methyl-pyrimidin-4-yl]-amine (CyPPA) and 3-Oxime-6,7-dichloro-1H-indole-2,3-dione (NS309) were previously described (Hougaard et al., 2007; Strøbaek et al., 2004). (4-Chlorophenyl)-[2-(3,5-dimethyl-pyrazol-1-yl)-9-methyl-9*H*-purin-6-yl]-amine (NS13001) is a novel compound (Eriksen et al., 2008) and its synthesis is described in SOM. Apamin was purchased from Sigma Aldrich. Lei-Dab7 was synthesized in the Sabatier laboratory by following published procedures (Shakkottai et al., 2001).

Animals

Procedures involving wild-type rats were conducted in strict accordance with the guidelines described in the Guide for Care and Use of Laboratory Animals, the policies adopted by the Society for Neuroscience, and the Danish Committee for Experiments on Animals. SCA2-58Q mice on C57/B6 background (Huynh et al., 2000) were kindly provided to our laboratory by Dr. Stefan Pulst (University of Utah) and have been used in our previous studies (Liu et al., 2009). In these mice the expression of human Atx2-58Q transgene is driven by the PC-specific L7/pcp2 promoter (Huynh et al., 2000). The mice were backcrossed to FVB/N background for at least 6 generations in our laboratory as previously described (Kasumu and Bezprozvanny, 2012; Kasumu et al., 2012). The SCA2-58Q (FVB) male hemizygotous mice were bred to wild-type (WT) FVB/N females to generate mixed litters. The pups were genotyped by PCR for the presence of human Atxn2 transgene and parallel experiments were performed with transgenic and wild-type littermates. All mice were housed in a temperature-controlled room at 22°C–24°C with a 12 hr light/dark cycle. Mice had access to standard chow and water ad lib. All procedures were approved by the Institutional Animal Care and Use Committee (IACUC) of the UT Southwestern Medical Center at Dallas in accordance with the National Institutes of Health guidelines for the Care and Use of Experimental Animals.

Cell Cultures

Human embryonic kidney (HEK) 293 cell lines stably expressing human SK1, SK2, and SK3 proteins have been previously described (Hougaard et al., 2009). Cells were cultured in Dulbecco's modified Eagle's medium (DMEM, GIBCO, Life Technologies, Nærum, Denmark) enriched with 10% fetal calf serum (FCS, GIBCO) at 37°C and 5% CO_2. One day prior to electrophysiological experiments, the cells (~75% confluency) were washed once with phosphate buffered saline (PBS), harvested by TrypLE Express (GIBCO) treatment, and transferred to Petri dishes containing cover 3.5 mm diameter coverslips (VWR international, Herlev, Denmark).

Recordings of Recombinant SK Channel Activity

SK-mediated membrane currents were recorded at room temperature using the inside-out configuration of the patch-clamp technique as previously described (Hougaard et al., 2007). Glass patch pipettes of 2 MΩ resistance were used in recordings using EPC-9 amplifier and Pulse software (HEKA, Lambrecht, Germany). In all experiments a solution with a high K^+ concentration was applied to the extracellular side of the membrane (in mM): 154 KCl, 2 $CaCl_2$, 1 $MgCl_2$, and 10 HEPES, pH adjusted to 7.4 with 1 M KOH. The intracellular solutions contained (in mM): 154 KCl, 10 HEPES, 10 EGTA, or a combination of EGTA and NTA (10 mM in total). Concentrations of $MgCl_2$ and $CaCl_2$ required to obtain the desired free concentrations (Mg^{2+} always 1 mM, Ca^{2+} 0.01–10 μM) were calculated (EqCal, Cambridge, UK) and added. The intracellular solutions were adjusted to pH 7.2 with 1 M KOH. The currents were elicited by applying a 200 ms linear voltage ramp from −80 to +80 mV every 5 s from a holding potential of 0 mV.

Recordings of Spontaneous PC Activity in Rat Cerebellar Slices

The recordings of PC activity from rat cerebellar slices were performed essentially as described (Kaffashian et al., 2011). Briefly, Sprague-Dawley rats

(14–18 days old; Taconic, Ry, Denmark) were decapitated and brains rapidly dissected out into ice-cold artificial CSF (aCSF) of the following composition (in mM): 124 NaCl, 4 KCl, 8 $MgSO_4$, 2.5 $CaCl_2$, 1.25 NaH_2PO_4, 26 $NaHCO_3$, 11 glucose, saturated with 95% O_2/5% CO_2. Parasagittal cerebellar slices (300 μm) were cut using a vibrating tissue slicer (VT1200 Leica, Ballerup, Denmark) and placed in a home-made holding chamber at room temperature in aCSF (composition like above except that $MgSO_4$ was reduced to 1.2 mM), bubbled with 95% O_2/5% CO_2. Slices were left to recover for a minimum of 1 hr prior to experiments. Individual slices were transferred to a submersion-style recording chamber (Luigs & Neumann Ratingen, Germany) and perfused at 2 ml/min with aCSF maintained at 30°C using a feedback-controlled heater (Warner Instruments, Hamden, CT). PCs for whole-cell current-clamp recordings were visualized at 40× using an upright Olympus microscope (BX51WI) equipped with oblique illumination. Patch pipettes of resistance 3–7 MΩ were filled with the pipette solutions containing (in mM): 135 CH_3KSO_4, 10 KCl, 10 HEPES, 1 $MgCl_2$, 2 Na_2-ATP, 0.4 Na-GTP, pH 7.2 with 1 M KOH. Following high resistance seal formation the membrane was ruptured by suction and recordings were performed using an EPC-9 amplifier (HEKA, Lambrecht, Germany). Experimental control, data acquisition, and basic analyses were done with the Patchmaster (HEKA) software package.

Recordings of Spontaneous PC Activity in Mouse Cerebellar Slices

Recordings of spontaneous PC activity from WT and 58Q mice at 24 weeks of age were performed as previously described (Kasumu et al., 2012). Briefly, the mice were anesthetized with a ketamine/xylazine cocktail and transcardially perfused with ice-cold aCSF containing (mM) 85 NaCl, 24 $NaHCO_3$, 25 glucose, 2.5 KCl, 0.5 $CaCl_2$, 4 $MgCl_2$, 1 NaH_2PO_4, 75 sucrose. Solutions were equilibrated with 95% O_2/5% CO_2. Subsequently, the cerebellum was dissected and 300 μm thick sagittal slices were made with a VT1200S vibratome (Leica). Slices were allowed to recover in aCSF containing (in mM) 119 NaCl, 26 $NaHCO_3$, 11 glucose, 2.5 KCl, 2.5 $CaCl_2$, 1.3 $MgCl_2$, 1 NaH_2PO_4 at 35°C for 30 min and then transferred to room temperature before recordings were made. The external bath used for recording was the same as the recovery aCSF in addition to containing 100 μM picrotoxin (PTX) and 10 μM 6,7-dinitroquinoxaline-2,3-dione (DNQX), equilibrated with 95% O_2/5% CO_2. All recordings were made within 5 hr after dissection. The recording chamber was heated to 34°C–35°C using PH1 heated holder (Warner Instruments, Hamden, CT). Loose-patch recordings were made according to (Häusser and Clark, 1997; Smith and Otis, 2003; Kasumu et al., 2012) to evaluate spontaneous activity of PCs. Briefly, 1–3 MΩ glass pipettes were filled with the internal solution containing 140 mM NaCl buffered with 10 mM HEPES pH 7.3 and held at 0 mV. A loose patch (<100 MΩ) configuration was established at the PC soma as close to the axon hillock as possible. Spontaneous action potential currents were recorded for 5–60 min from each cell using Axon Multiclamp 700B amplifier (Molecular Devices, Sunnyvale, CA). The 5 min recordings were analyzed for tonic or burst firing as we previously described (Kasumu et al., 2012). Cells were characterized as firing tonically if they fired repetitive nonhalting spike trains for 5 min. A cell was characterized as bursting if it had more than 5% of the interspike intervals that fell outside of 3 SD from the mean of all interspike intervals in that cell. The analysis of instantaneous firing rates was performed using Clampfit 10.2 (Molecular Devices). Data was plotted as the instantaneous firing rate every 2 s for the entire recording duration. From the plot of firing rates, bursting PCs were further categorized into two groups. Persistently bursting PCs were identified by a continuous presentation of bursts, each separated from the next by a period of silence (<1 min), throughout the duration of the recording. Transiently bursting PCs were identified by the presence of long periods of relatively constant tonic firing separated by short intermittent bursts. Once a burst firing pattern was observed during the first 5 min of recordings, the bath solution was switched to aCSF containing 5 μM NS309 or 5 μM CyPPA for at least 15 min to determine the effect of the compound on the firing pattern of that PC.

Motor Coordination Assessments in Mice

The drug feeding protocol was adapted from our previous study (Liu et al., 2009). NS13001 (30 mg/kg) or CyPPA (10 mg/kg) was suspended in the vehicle (0.5% HPMC-corn flour suspension). The mice were fed orally 5 consecutive days (Monday to Friday) with 2 rest days (Saturday and Sunday) for 3 consecutive weeks starting at 9 months of age. Control groups of mice were fed with the vehicle (0.5% HPMC-corn flour suspension) alone. Rotarod and beamwalk tasks were used to assess motor coordination as previously described (Kasumu et al., 2012; Liu et al., 2009). At baseline (prior to drug feeding), mice were trained on the beamwalk task to traverse three separate beams of differing diameters. A round plastic 17 mm beam, a round plastic 11 mm beam, and a wooden square 5 mm beam were used for training. Mice were given three consecutive training trials on 3 consecutive days on each beam. On the third day, the mean latencies to traverse the entire length of the 11 mm and 5 mm beams were recorded and analyzed for every animal in all six groups. After testing on the beamwalk task, mice were given a 3 day wait period and subsequently trained on the accelerating rotarod task. Mice were trained to walk on a rotating rod accelerating at 0.2 rpm. Mice were trained for 4 consecutive days with three consecutive trials per day. The mean latency to fall off the accelerating rod was recorded and analyzed for every animal in all six groups. After baseline testing, mice were fed for 3 consecutive weeks with the allotted compounds. Following drug feeding, mice were left alone for 3 days and then retested in motor tasks. Specifically, mice were trained on the beamwalk with three trials per beam on day 1 and tested on day 2. After a 3 day waiting period, mice were trained on the accelerating rotarod (Columbus Instruments, Columbus, OH) with three consecutive trials on day 6 and tested on day 7.

Dark Cell Degeneration Analyses

Quantification of dark cell degeneration (DCD) status was performed as previously described (Kasumu and Bezprozvanny, 2012; Kasumu et al., 2012). Briefly, five to six mice in each group were sacrificed at 13 months of age. Mice were euthanized with pentobarbital and transcardially perfused with PBS followed by 2% paraformaldehyde/2% glutaraldehyde in 0.1 M cacodylate buffer. The cerebellum was dissected out and cut into 1 mm^3 sagittal sections and postfixed in 1% osmium tetroxide. The specimen were subsequently stained en bloc with aqueous 1% uranyl acetate and lead citrate, dehydrated through a graded ethanol series, and embedded in EMbed 812 resin. Each cerebellum was cut into thinner 70 μm-thick sections and placed on copper grids, which were stained with aqueous 2% uranyl acetate and lead citrate. Sections from each animal were examined on a FEI Tecnai G2 Spirit Biotwin transmission electron microscope operated at 120 kV. Digital images were captured with a SIS Morada 11 megapixel side mount CCD camera. At least five mice were analyzed per group with two grids made from different areas of the sections. PCs were judged to be in one of three stages—normal, moderate, or severe. Normal PCs are spherical in shape and have regular alignment in the PC layer. The nucleus is also distinctly darker than the cytosol. Moderately degenerated PCs have slight shrinkage and moderately electron-dense cytosol that is almost as dark as nucleus. Severely degenerated PCs have markedly shrunken and electron-dense cytosol with similarly darkened nucleus. These PCs are usually not regularly aligned in the PC layer. The processing of samples for DCD analyses were performed by an investigator that was blind to genotype and treatment group. Quantification of DCD status of PCs was performed by an investigator that was also blind to mouse genotype and treatment group. The average percentage of normal, moderate and severely degenerated cells was calculated for each treatment group and plotted.

Statistical Analyses

Differences between groups were judged by a two-tailed Student's unpaired t test using a significance level of 0.05.

SUPPLEMENTAL INFORMATION

Supplemental Information includes five figures and Supplemental Experimental Procedures and can be found with this article online at http://dx.doi.org/10.1016/j.chembiol.2012.07.013.

ACKNOWLEDGMENTS

We thank Leah Taylor for administrative assistance. Vibeke Meyland-Smith and Susanne Kalf Hansen are greatly acknowledged for their help with patch clamp experiments and preparation of cerebellar slices. Lise Lauenborg is acknowledged for help with the synthesis of CyPPA and NS13001. Dr. Nicolas

Andreotti is thanked for his help with the synthesis of LeiDab-7. A.W.K. is a Howard Hughes Medical Institute Med into Grad scholar. I.B. is a holder of the Carl J. and Hortense M. Thomsen Chair in Alzheimer's Disease Research. This study is supported in part by a contract with Neurosearch A/S (to P.C., L.C.B.R., and I.B.), by the NIH Grants R01NS056224, R01NS38082 and R01NS074376 (to I.B.), Welch Foundation grant I-1754 (to I.B.), and by the contract with the Russian Ministry of Science 14.740.11.0924 (to I.B.). C.H., F.R., T.A.J., B.L.E., D.S., P.C., and L.C.B.R. are employees and shareholders of Neurosearch A/S.

Received: May 1, 2012
Revised: June 25, 2012
Accepted: July 10, 2012
Published: October 25, 2012

REFERENCES

Adelman, J.P., Maylie, J., and Sah, P. (2012). Small-conductance Ca2+-activated K+ channels: form and function. Annu. Rev. Physiol. *74*, 245–269.

Alviña, K., and Khodakhah, K. (2010a). KCa channels as therapeutic targets in episodic ataxia type-2. J. Neurosci. *30*, 7249–7257.

Alviña, K., and Khodakhah, K. (2010b). The therapeutic mode of action of 4-aminopyridine in cerebellar ataxia. J. Neurosci. *30*, 7258–7268.

Becker, C., Jick, S.S., and Meier, C.R. (2008). Use of antihypertensives and the risk of Parkinson disease. Neurology *70*, 1438–1444.

Benítez, B.A., Belálcazar, H.M., Anastasía, A., Mamah, D.T., Zorumski, C.F., Mascó, D.H., Herrera, D.G., and de Erausquin, G.A. (2011). Functional reduction of SK3-mediated currents precedes AMPA-receptor-mediated excitotoxicity in dopaminergic neurons. Neuropharmacology *60*, 1176–1186.

Bezprozvanny, I., and Klockgether, T. (2010). Therapeutic prospects for spinocerebellar ataxia type 2 and 3. Drugs Future *34*, 991–999.

Bishop, M.W., Chakraborty, S., Matthews, G.A., Dougalis, A., Wood, N.W., Festenstein, R., and Ungless, M.A. (2010). Hyperexcitable substantia nigra dopamine neurons in PINK1- and HtrA2/Omi-deficient mice. J. Neurophysiol. *104*, 3009–3020.

Bond, C.T., Sprengel, R., Bissonnette, J.M., Kaufmann, W.A., Pribnow, D., Neelands, T., Storck, T., Baetscher, M., Jerecic, J., Maylie, J., et al. (2000). Respiration and parturition affected by conditional overexpression of the Ca2+-activated K+ channel subunit, SK3. Science *289*, 1942–1946.

Callizot, N., Guénet, J.L., Baillet, C., Warter, J.M., and Poindron, P. (2001). The frissonnant mutant mouse, a model of dopamino-sensitive, inherited motor syndrome. Neurobiol. Dis. *8*, 447–458.

Cao, Y., Dreixler, J.C., Roizen, J.D., Roberts, M.T., and Houamed, K.M. (2001). Modulation of recombinant small-conductance Ca(2+)-activated K(+) channels by the muscle relaxant chlorzoxazone and structurally related compounds. J. Pharmacol. Exp. Ther. *296*, 683–689.

Carlson, K.M., Andresen, J.M., and Orr, H.T. (2009). Emerging pathogenic pathways in the spinocerebellar ataxias. Curr. Opin. Genet. Dev. *19*, 247–253.

Chan, C.S., Gertler, T.S., and Surmeier, D.J. (2009). Calcium homeostasis, selective vulnerability and Parkinson's disease. Trends Neurosci. *32*, 249–256.

Chan, C.S., Gertler, T.S., and Surmeier, D.J. (2010). A molecular basis for the increased vulnerability of substantia nigra dopamine neurons in aging and Parkinson's disease. Mov. Disord. *25* (*Suppl 1*), S63–S70.

Cingolani, L.A., Gymnopoulos, M., Boccaccio, A., Stocker, M., and Pedarzani, P. (2002). Developmental regulation of small-conductance Ca2+-activated K+ channel expression and function in rat Purkinje neurons. J. Neurosci. *22*, 4456–4467.

Custer, S.K., Garden, G.A., Gill, N., Rueb, U., Libby, R.T., Schultz, C., Guyenet, S.J., Deller, T., Westrum, L.E., Sopher, B.L., and La Spada, A.R. (2006). Bergmann glia expression of polyglutamine-expanded ataxin-7 produces neurodegeneration by impairing glutamate transport. Nat. Neurosci. *9*, 1302–1311.

de Solages, C., Szapiro, G., Brunel, N., Hakim, V., Isope, P., Buisseret, P., Rousseau, C., Barbour, B., and Léna, C. (2008). High-frequency organization and synchrony of activity in the Purkinje cell layer of the cerebellum. Neuron *58*, 775–788.

Drion, G., Seutin, V., and Sepulchre, R. (2012). Mitochondrion- and endoplasmic reticulum-induced SK channel dysregulation as a potential origin of the selective neurodegeneration in Parkinson's disease. In Systems Biology of Parkinson's Disease, P. Wellstead and M. Cloutier, eds. (NY: Springer Science & Business Media), pp. 57–79.

Eriksen, B.L., Sorensen, U.S., Hougaard, C., Peters, D., Johansen, T.H., and Christophersen, P. February 2008. Purinyl derivatives and their use as potassium channel modulators. WIPO patent WO 2008/116909 A1.

Hammond, R.S., Bond, C.T., Strassmaier, T., Ngo-Anh, T.J., Adelman, J.P., Maylie, J., and Stackman, R.W. (2006). Small-conductance Ca2+-activated K+ channel type 2 (SK2) modulates hippocampal learning, memory, and synaptic plasticity. J. Neurosci. *26*, 1844–1853.

Häusser, M., and Clark, B.A. (1997). Tonic synaptic inhibition modulates neuronal output pattern and spatiotemporal synaptic integration. Neuron *19*, 665–678.

Heck, D.H., Thach, W.T., and Keating, J.G. (2007). On-beam synchrony in the cerebellum as the mechanism for the timing and coordination of movement. Proc. Natl. Acad. Sci. USA *104*, 7658–7663.

Herrik, K.F., Redrobe, J.P., Holst, D., Hougaard, C., Sandager-Nielsen, K., Nielsen, A.N., Ji, H., Holst, N.M., Rasmussen, H.B., Nielsen, E.O., et al. (2012). CyPPA, a positive SK3/SK2 modulator, reduces activity of dopaminergic neurons, inhibits dopamine release, and counteracts hyperdopaminergic behaviors induced by methylphenidate. Front Pharmacol *3*, 11.

Hosy, E., Piochon, C., Teuling, E., Rinaldo, L., and Hansel, C. (2011). SK2 channel expression and function in cerebellar Purkinje cells. J. Physiol. *589*, 3433–3440.

Hougaard, C., Eriksen, B.L., Jørgensen, S., Johansen, T.H., Dyhring, T., Madsen, L.S., Strøbaek, D., and Christophersen, P. (2007). Selective positive modulation of the SK3 and SK2 subtypes of small conductance Ca2+-activated K+ channels. Br. J. Pharmacol. *151*, 655–665.

Hougaard, C., Jensen, M.L., Dale, T.J., Miller, D.D., Davies, D.J., Eriksen, B.L., Strøbaek, D., Trezise, D.J., and Christophersen, P. (2009). Selective activation of the SK1 subtype of human small-conductance Ca2+-activated K+ channels by 4-(2-methoxyphenylcarbamoyloxymethyl)-piperidine-1-carboxylic acid tert-butyl ester (GW542573X) is dependent on serine 293 in the S5 segment. Mol. Pharmacol. *76*, 569–578.

Huynh, D.P., Figueroa, K., Hoang, N., and Pulst, S.M. (2000). Nuclear localization or inclusion body formation of ataxin-2 are not necessary for SCA2 pathogenesis in mouse or human. Nat. Genet. *26*, 44–50.

Ito, M. (2002). Historical review of the significance of the cerebellum and the role of Purkinje cells in motor learning. Ann. N Y Acad. Sci. *978*, 273–288.

Jacobsen, J.P., Weikop, P., Hansen, H.H., Mikkelsen, J.D., Redrobe, J.P., Holst, D., Bond, C.T., Adelman, J.P., Christophersen, P., and Mirza, N.R. (2008). SK3 K+ channel-deficient mice have enhanced dopamine and serotonin release and altered emotional behaviors. Genes Brain Behav. *7*, 836–848.

Jacobsen, J.P., Redrobe, J.P., Hansen, H.H., Petersen, S., Bond, C.T., Adelman, J.P., Mikkelsen, J.D., and Mirza, N.R. (2009). Selective cognitive deficits and reduced hippocampal brain-derived neurotrophic factor mRNA expression in small-conductance calcium-activated K+ channel deficient mice. Neuroscience *163*, 73–81.

Johnson, S.W., and Wu, Y.N. (2004). Multiple mechanisms underlie burst firing in rat midbrain dopamine neurons in vitro. Brain Res. *1019*, 293–296.

Kaffashian, M., Shabani, M., Goudarzi, I., Behzadi, G., Zali, A., and Janahmadi, M. (2011). Profound alterations in the intrinsic excitability of cerebellar Purkinje neurons following neurotoxin 3-acetylpyridine (3-AP)-induced ataxia in rat: new insights into the role of small conductance K+ channels. Physiol. Res. *60*, 355–365.

Kasumu, A., and Bezprozvanny, I. (2012). Deranged calcium signaling in Purkinje cells and pathogenesis in spinocerebellar ataxia 2 (SCA2) and other ataxias. Cerebellum *11*, 630–639.

Kasumu, A., Liang, X., Egorova, P., Vorontsova, D., and Bezprozvanny, I. (2012). Chronic suppression of inositol 1, 4,5-triphosphate receptor-mediated calcium signaling in cerebellar Purkinje cells alleviates pathological phenotype in spinocerebellar ataxia 2 mice. J. Neurosci. *32*, 12786–12796.

Klockgether, T., Lüdtke, R., Kramer, B., Abele, M., Bürk, K., Schöls, L., Riess, O., Laccone, F., Boesch, S., Lopes-Cendes, I., et al. (1998). The natural history of degenerative ataxia: a retrospective study in 466 patients. Brain *121*, 589–600.

Kuiper, E.F.E., Nelemans, A., Luiten, P.G.M., Nijholt, I.M., Dolga, A.M., and Eisel, U.L.M. (2012). KCa2 and KCa3 channels in learning and memory processes, and neurodegeneration. Front Pharmacol. *3*, 107.

Kuznetsov, A.S., Kopell, N.J., and Wilson, C.J. (2006). Transient high-frequency firing in a coupled-oscillator model of the mesencephalic dopaminergic neuron. J. Neurophysiol. *95*, 932–947.

Lastres-Becker, I., Rüb, U., and Auburger, G. (2008). Spinocerebellar ataxia 2 (SCA2). Cerebellum *7*, 115–124.

Liu, J., Tang, T.S., Tu, H., Nelson, O., Herndon, E., Huynh, D.P., Pulst, S.M., and Bezprozvanny, I. (2009). Deranged calcium signaling and neurodegeneration in spinocerebellar ataxia type 2. J. Neurosci. *29*, 9148–9162.

Llinás, R., and Sugimori, M. (1980a). Electrophysiological properties of in vitro Purkinje cell dendrites in mammalian cerebellar slices. J. Physiol. *305*, 197–213.

Llinás, R., and Sugimori, M. (1980b). Electrophysiological properties of in vitro Purkinje cell somata in mammalian cerebellar slices. J. Physiol. *305*, 171–195.

Louis, E.D., Benito-León, J., and Bermejo-Pareja, F.; Neurological Disorders in Central Spain (NEDICES) Study Group. (2009). Antihypertensive agents and risk of Parkinson's disease, essential tremor and dementia: a population-based prospective study (NEDICES). Neuroepidemiology *33*, 286–292.

Maltecca, F., Magnoni, R., Cerri, F., Cox, G.A., Quattrini, A., and Casari, G. (2009). Haploinsufficiency of AFG3L2, the gene responsible for spinocerebellar ataxia type 28, causes mitochondria-mediated Purkinje cell dark degeneration. J. Neurosci. *29*, 9244–9254.

Matilla-Dueñas, A., Sanchez, I., Corral-Juan, M., Davalos, A., Alvarez, R., and Latorre, P. (2010). Cellular and molecular pathways triggering neurodegeneration in the spinocerebellar ataxias. Cerebellum *9*, 148–166.

Mpari, B., Sreng, L., Manrique, C., and Mourre, C. (2010). KCa2 channels transiently downregulated during spatial learning and memory in rats. Hippocampus *20*, 352–363.

Nam, S.C., and Hockberger, P.E. (1997). Analysis of spontaneous electrical activity in cerebellar Purkinje cells acutely isolated from postnatal rats. J. Neurobiol. *33*, 18–32.

Orr, H.T., and Zoghbi, H.Y. (2007). Trinucleotide repeat disorders. Annu. Rev. Neurosci. *30*, 575–621.

Patkó, T., Vassias, I., Vidal, P.P., and De Waele, C. (2003). Modulation of the voltage-gated sodium- and calcium-dependent potassium channels in rat vestibular and facial nuclei after unilateral labyrinthectomy and facial nerve transsection: an in situ hybridization study. Neuroscience *117*, 265–280.

Pedarzani, P., McCutcheon, J.E., Rogge, G., Jensen, B.S., Christophersen, P., Hougaard, C., Strøbaek, D., and Stocker, M. (2005). Specific enhancement of SK channel activity selectively potentiates the after hyperpolarizing current I(AHP) and modulates the firing properties of hippocampal pyramidal neurons. J. Biol. Chem. *280*, 41404–41411.

Person, A.L., and Raman, I.M. (2012). Purkinje neuron synchrony elicits time-locked spiking in the cerebellar nuclei. Nature *481*, 502–505.

Pulst, S.M., Nechiporuk, A., Nechiporuk, T., Gispert, S., Chen, X.N., Lopes-Cendes, I., Pearlman, S., Starkman, S., Orozco-Diaz, G., Lunkes, A., et al. (1996). Moderate expansion of a normally Biallelic trinucleotide repeat in spinocerebellar ataxia type 2. Nat. Genet. *14*, 269–276.

Raman, I.M., and Bean, B.P. (1997). Resurgent sodium current and action potential formation in dissociated cerebellar Purkinje neurons. J. Neurosci. *17*, 4517–4526.

Raman, I.M., and Bean, B.P. (1999). Ionic currents underlying spontaneous action potentials in isolated cerebellar Purkinje neurons. J. Neurosci. *19*, 1663–1674.

Rinaldo, L., and Hansel, C. (2010). Ataxias and cerebellar dysfunction: involvement of synaptic plasticity deficits? Funct. Neurol. *25*, 135–139.

Ristori, G., Romano, S., Visconti, A., Cannoni, S., Spadaro, M., Frontali, M., Pontieri, F.E., Vanacore, N., and Salvetti, M. (2010). Riluzole in cerebellar ataxia: a randomized, double-blind, placebo-controlled pilot trial. Neurology *74*, 839–845.

Ritz, B., Rhodes, S.L., Qian, L., Schernhammer, E., Olsen, J.H., and Friis, S. (2010). L-type calcium channel blockers and Parkinson disease in Denmark. Ann. Neurol. *67*, 600–606.

Ross, O.A., Rutherford, N.J., Baker, M., Soto-Ortolaza, A.I., Carrasquillo, M.M., DeJesus-Hernandez, M., Adamson, J., Li, M., Volkening, K., Finger, E., et al. (2011). Ataxin-2 repeat-length variation and neurodegeneration. Hum. Mol. Genet. *20*, 3207–3212.

Sabatini, B.L., Maravall, M., and Svoboda, K. (2001). Ca(2+) signaling in dendritic spines. Curr. Opin. Neurobiol. *11*, 349–356.

Sailer, C.A., Hu, H., Kaufmann, W.A., Trieb, M., Schwarzer, C., Storm, J.F., and Knaus, H.G. (2002). Regional differences in distribution and functional expression of small-conductance Ca2+-activated K+ channels in rat brain. J. Neurosci. *22*, 9698–9707.

Sailer, C.A., Kaufmann, W.A., Marksteiner, J., and Knaus, H.G. (2004). Comparative immunohistochemical distribution of three small-conductance Ca2+-activated potassium channel subunits, SK1, SK2, and SK3 in mouse brain. Mol. Cell. Neurosci. *26*, 458–469.

Sankaranarayanan, A., Raman, G., Busch, C., Schultz, T., Zimin, P.I., Hoyer, J., Köhler, R., and Wulff, H. (2009). Naphtho[1,2-d]thiazol-2-ylamine (SKA-31), a new activator of KCa2 and KCa3.1 potassium channels, potentiates the endothelium-derived hyperpolarizing factor response and lowers blood pressure. Mol. Pharmacol. *75*, 281–295.

Shakkottai, V.G., Regaya, I., Wulff, H., Fajloun, Z., Tomita, H., Fathallah, M., Cahalan, M.D., Gargus, J.J., Sabatier, J.M., and Chandy, K.G. (2001). Design and characterization of a highly selective peptide inhibitor of the small conductance calcium-activated K+ channel, SkCa2. J. Biol. Chem. *276*, 43145–43151.

Shakkottai, V.G., Chou, C.H., Oddo, S., Sailer, C.A., Knaus, H.G., Gutman, G.A., Barish, M.E., LaFerla, F.M., and Chandy, K.G. (2004). Enhanced neuronal excitability in the absence of neurodegeneration induces cerebellar ataxia. J. Clin. Invest. *113*, 582–590.

Shakkottai, V.G., do Carmo Costa, M., Dell'Orco, J.M., Sankaranarayanan, A., Wulff, H., and Paulson, H.L. (2011). Early changes in cerebellar physiology accompany motor dysfunction in the polyglutamine disease spinocerebellar ataxia type 3. J. Neurosci. *31*, 13002–13014.

Shepard, P.D., and Bunney, B.S. (1988). Effects of apamin on the discharge properties of putative dopamine-containing neurons in vitro. Brain Res. *463*, 380–384.

Simon-Sanchez, J., Hanson, M., Singleton, A., Hernandez, D., McInerney, A., Nussbaum, R., Werner, J., Gallardo, M., Weiser, R., Gwinn-Hardy, K., et al. (2005). Analysis of SCA-2 and SCA-3 repeats in Parkinsonism: evidence of SCA-2 expansion in a family with autosomal dominant Parkinson's disease. Neurosci. Lett. *382*, 191–194.

Simon, K.C., Gao, X., Chen, H., Schwarzschild, M.A., and Ascherio, A. (2010). Calcium channel blocker use and risk of Parkinson's disease. Mov. Disord. *25*, 1818–1822.

Smith, S.L., and Otis, T.S. (2003). Persistent changes in spontaneous firing of Purkinje neurons triggered by the nitric oxide signaling cascade. J. Neurosci. *23*, 367–372.

Stackman, R.W., Hammond, R.S., Linardatos, E., Gerlach, A., Maylie, J., Adelman, J.P., and Tzounopoulos, T. (2002). Small conductance Ca2+-activated K+ channels modulate synaptic plasticity and memory encoding. J. Neurosci. *22*, 10163–10171.

Stackman, R.W., Jr., Bond, C.T., and Adelman, J.P. (2008). Contextual memory deficits observed in mice overexpressing small conductance Ca2+-activated K+ type 2 (KCa2.2, SK2) channels are caused by an encoding deficit. Learn. Mem. *15*, 208–213.

Stocker, M. (2004). Ca(2+)-activated K+ channels: molecular determinants and function of the SK family. Nat. Rev. Neurosci. *5*, 758–770.

Stocker, M., and Pedarzani, P. (2000). Differential distribution of three Ca(2+)-activated K(+) channel subunits, SK1, SK2, and SK3, in the adult rat central nervous system. Mol. Cell. Neurosci. *15*, 476–493.

Strøbaek, D., Teuber, L., Jørgensen, T.D., Ahring, P.K., Kjaer, K., Hansen, R.S., Olesen, S.P., Christophersen, P., and Skaaning-Jensen, B. (2004). Activation of human IK and SK Ca2+ -activated K+ channels by NS309 (6,7-dichloro-1H-indole-2,3-dione 3-oxime). Biochim. Biophys. Acta *1665*, 1–5.

Surmeier, D.J. (2007). Calcium, ageing, and neuronal vulnerability in Parkinson's disease. Lancet Neurol. *6*, 933–938.

Surmeier, D.J., Guzman, J.N., and Sanchez-Padilla, J. (2010). Calcium, cellular aging, and selective neuronal vulnerability in Parkinson's disease. Cell Calcium *47*, 175–182.

Vick, K.A., 4th, Guidi, M., and Stackman, R.W., Jr. (2010). In vivo pharmacological manipulation of small conductance Ca(2+)-activated K(+) channels influences motor behavior, object memory and fear conditioning. Neuropharmacology *58*, 650–659.

Walter, J.T., Alviña, K., Womack, M.D., Chevez, C., and Khodakhah, K. (2006). Decreases in the precision of Purkinje cell pacemaking cause cerebellar dysfunction and ataxia. Nat. Neurosci. *9*, 389–397.

Womack, M., and Khodakhah, K. (2002). Active contribution of dendrites to the tonic and trimodal patterns of activity in cerebellar Purkinje neurons. J. Neurosci. *22*, 10603–10612.

Womack, M.D., and Khodakhah, K. (2003). Somatic and dendritic small-conductance calcium-activated potassium channels regulate the output of cerebellar Purkinje neurons. J. Neurosci. *23*, 2600–2607.

Zhang, M., Pascal, J.M., Schumann, M., Armen, R.S., and Zhang, J.F. (2012). Identification of the functional binding pocket for compounds targeting small-conductance Ca(2+)-activated potassium channels. Nat. Commun. *3*, 1021.